



## Development of methodology for assessing flowability of milk protein powders using shear failure testing device

Katelynn Palmer<sup>a</sup>, Ashutos Parhi<sup>a</sup>, Abhishek Shetty<sup>b</sup>, Venkateswarlu Sunkesula<sup>c</sup>,  
Prateek Sharma<sup>a,\*</sup>

<sup>a</sup> Nutrition, Dietetics and Food Sciences (NDFS) Department, Utah State University, 8700 Old Main Hill, Logan, UT 84322, USA

<sup>b</sup> Rheology Division, Anton Paar USA, Inc., Ashland, VA 23005, USA

<sup>c</sup> Idaho Milk Products, 2249 S Tiger Dr, Jerome, ID 83338, USA



### ARTICLE INFO

#### Keywords:

Milk protein powders  
Shear cell  
SEM  
Particle size  
Flowability

### ABSTRACT

Protein-rich milk powders can be susceptible to caking and clumping during manufacture and storage. A method was developed for objective and reliable assessment of their flowability, i.e., tendency of powders not to stick to the equipment surfaces. Milk protein powder (MPC 80) was subjected to three-point shear failure testing on a powder shear cell attached to a MCR302e rheometer. Flow function coefficients ( $ff_c$ ) were obtained after the Mohr circle analysis of pre-shear and shear-to-failure points. Due to their globular shape and significantly larger particle size (50–70  $\mu\text{m}$ ), milk protein powders exhibited more stick-slip phenomenon and lack of shear-to-failure points particularly at higher pre-shear (>6 kPa) and shearing normal stresses than the flat-shaped, smaller size (<20  $\mu\text{m}$ ) cohesive calcium carbonate powder ( $ff_c$  value 2.1 at 3.0 kPa). Absence of shear-to-failure points in milk protein powders was attributed to instant failure of the powder at higher normal stresses due to larger particle size and globular shape, which was avoided by lowering pre-shear (3, 6, and 9 kPa to 1, 3 and 6 kPa) and shearing normal stresses, increasing data capturing interval and optimizing shear speed. Reliable  $ff_c$  values at 3.0 kPa pre-shear normal stress, characterizing MPC 80 powder ( $4.6 \pm 0.4$ ) as easy flowing and MPI 85 as cohesive ( $3.7 \pm 0.5$ ) were obtained successfully using developed protocol.

### 1. Introduction

Protein-rich dairy powders can be an ideal source for fulfilling the nutritional requirements of the population (Khalesi and FitzGerald, 2021; Gaspard et al., 2021; Silva and O'Mahony, 2017). They are easy to package, carry and store, occupy a lesser volume than their whole, refrigerated shelf-stable counterparts, and have a reduced possibility of microbial contamination and growth during transportation and storage (Khalesi and FitzGerald, 2021; Schulze, 2008; Stavrou et al., 2020). Dried dairy products are a viable and safe alternative to fluid milk due to their attributes of nutritional retention, convenience, and broader functionality, all of which significantly enhance their ease of usage and consumer appreciation (Ji et al., 2016). However, powders can be prone to caking and clumping, which reduces flowability and causes hindrances during processing and storage (Boiarkina et al., 2016; Carpin et al., 2017; Foster et al., 2005). Caking can lead to inconsistent blends and poor rehydration characteristics, lowering consumer satisfaction with the final product. Several factors such as relative humidity,

temperature, physical state and morphology of lactose and protein, variability in composition, and the length of the storage period can influence the extent of caking (Carpin et al., 2017; Crowley et al., 2014; Foster et al., 2005).

Studying the rheological properties of food powders, and particularly the flow function coefficient ( $ff_c$ ) i.e., objective measurement of cohesion and flow tendencies of food powders, can assist the food industry in predicting powder flowability. Thus, leading to the optimization of the space required for transportation and storage, and enhancing sustainability of powder handling operations. This is beneficial for milk processing plants. Unlike powder products from pharmaceutical or other industries, dairy powders are highly susceptible to environmental conditions such as moisture and temperature, which affect the powder's flowability (Kamath et al., 1994; Stoklosa et al., 2012). This is because dairy powders are composed of multiple components (fat, protein, and lactose), therefore, are more reactive to environmental conditions, as compared with more robust inorganic powders e. g calcium carbonate powder. In addition to environmental conditions, the flow

\* Corresponding author.

E-mail address: [prateek.sharma@usu.edu](mailto:prateek.sharma@usu.edu) (P. Sharma).

characteristics of dairy powders are also affected by particle size, morphology, surface composition. Unlike homogenous, inorganic powdered products, the reactive nature of dairy powders can result in serious challenges such as caking and clumping, which reduces flowability and can negatively impact the space required for processing, packaging and storage (Foster et al., 2005; Ji et al., 2016; Wang et al., 2016a). Therefore, measurement of the *ffc* of the dairy powders can assist in hopper design, thus making the process more sustainable by optimizing the available resources (Carpin et al., 2017; Crowley et al., 2014; Wang et al., 2016a). Additionally, understanding the flow behavior of specific powders can provide detailed understanding of the variables that are essential for designing and developing the conveyor systems for food powders with variable compositional parameters (Boiarkina et al., 2016; Crowley et al., 2014; Schulze, 2008).

A shear cell is ideal for analyzing high to moderately cohesive powders. In addition, the general shear cell methodology provides useful insight into the powder's flow behavior under small load/stress conditions such as flowing through hopper or storing in silos. This is especially significant for food products vulnerable to caking and clumping during storage (Schulze, 2008; Wang et al., 2016a). The shear cell method involves three major steps: consolidation, pre-shear, and shear. The pre-shear minimizes the impact of prior history, while the shearing phase subjects the powders to a combined effect of the normal stress consolidation and shear stresses. The response of the powders is recorded through the shear failure diagrams (Bagga et al., 2012; Schulze, 2008; Wang et al., 2016a).

The shear cell technique has been successfully applied in studying the flow behavior of inorganic powders, specifically the pharmaceutical powders (Wang et al., 2016a, 2016b). Calcium carbonate powder has been used previously as a standard or reference for characterizing the powder flowability with a ring shear testing method for round robin testing (Akers, 1990; Parrella et al., 2008). The powder is cohesive and provides consistent results. In addition,  $\text{CaCO}_3$  powders consist of rigid particles, and do not conform to orientation phenomena during the shearing process, even at higher consolidation stresses, making it a reliable source for comparing the flow curves resulting from shearing of other powders.

However, there are a few studies on the use of shear cell method for determining the flow behavior of milk protein powders (Crowley et al., 2014; Fournaise et al., 2020). None of these studies provided details of the actual testing protocol/methodology (pre-shear and shearing consolidation stresses, shear failure points, rotational speed), nor gave exact details of the Mohr circle analysis. Additionally, there is no literature available in relation to obtaining reliable shear-to-failure points and estimation of flow function coefficient (*ffc*) for relatively less cohesive dairy powders. Prior research has also not included shear-to-failure diagrams that could further explain the shear failure mechanism. Shear cells using the three-point shear failure testing model are typically used for more cohesive powders. However, dairy powders are generally less cohesive due to their larger particle size range of 85–250  $\mu\text{m}$  (Tuohy et al., 1989). As a result, the previously researched methods were not effective in determining an approach to analyze the milk protein powders. The lack of this data makes it challenging for the food industry to take advantage of this excellent method in obtaining a more detailed understanding of powder rheology. Since prior research has predominantly characterized non-food or pharmaceutical cohesive powders (Wang et al., 2016a, 2016b), these methods may, or may not, conform when food powders are subjected to a similar protocol, necessitating a thorough study involving a new method development. Schulze (2008) mentioned that stick-slip, which is one of the predominant phenomena involving powders, primarily depends on the material properties and testing conditions. Hence, it is necessary to develop a methodology capable of gathering a deeper understanding of the flow behavior of food powders using a shear cell. Although air bearing rheometers in conjunction with powder accessories have been used in the past for various powder characterization studies (Chang et al., 2020;

Hartig et al., 2022; Iams et al., 2022; Jange et al., 2020; Mishra et al., 2020, 2022; Ramaraju et al., 2022; Zhao et al., 2021) the shear cell attachment has not yet been explored on dairy powders. Testing food powders in varying temperature and relative humidity will provide useful insights of the flowability behavior, and the shear cell can now be equipped with an attached temperature and relative humidity cabinet. However, the absence of reliable test methods for measuring flowability of dairy powders leads to underutilization of these attachments.

Regardless of powder type, traditional rheology methods available in literature do not provide detailed information about the analysis used for calculating the *ffc* and other flow parameters in a shear cell (Schulze, 2008). The primary hypothesis of this study was that food powders require a highly specific protocol for measuring their flow behavior in a shear cell. Based upon this, the current study focused on developing a methodology to successfully analyze less cohesive food protein powders for flowability using a shear cell. The study experimented with two dairy powders: milk protein concentrate (MPC 80) and milk protein isolate (MPI 85). The powders were subjected to two main test protocols, distinguished by the pre-shear normal stresses (3, 6, and 9 kPa and 1, 3, and 6 kPa). The second phase of testing studied impact of four shear speeds (0.003, 0.005, 0.006, and 0.009 rpm) and two different measurement point durations (0.5 s and 2 s) on the quality and reliability of flowability data. The results obtained from the milk powders were compared with the analysis results from the standard calcium carbonate powder as completed with the default instrument procedures. Furthermore, the morphological properties, and particle sizes of the powders were measured and correlated with the flowability.

## 2. Materials and methods

### 2.1. Milk protein powders

Two commercial milk protein powders: milk protein concentrate (MPC 80) and milk protein isolate (MPI 85), were procured from Idaho Milk Products (Jerome, ID). The powders were placed in an airtight container to prevent moisture exposure during the duration of the study.

### 2.2. Measurement of physicochemical properties

#### 2.2.1. Water activity

The water activity of the powders was measured at 22 °C using a water activity meter (Aqua Lab PRE, Meter food, Pullman, WA). All the measurements were performed in triplicate.

#### 2.2.2. Moisture content

The moisture content was measured in a rapid moisture analyzer (CEM Smart System 5, CEM Corporation Matthews, NC). The measurements were performed in triplicate.

#### 2.2.3. Bulk density

The bulk density was measured in terms of the loose and packed bulk densities. For measuring the loose density, a 100 mL graduated plastic cylinder was weighed and tared. Then, the graduated cylinder was manually filled with powder to the 100 mL mark and the weight was noted. The density was calculated based on the weight of the powder contained in the 100 mL volume. Subsequently, the packed (tapped) density was calculated by tapping the cylinder containing the powder 100 times on the benchtop. After 100 taps, the tapping ceased, and the weight of the powder was measured and change in powder volume noted. The packed density was calculated by dividing weight of the tapped powder by the volume of the powder in the cylinder (Crowley et al., 2014). Both the measurements were performed in duplicate.

#### 2.2.4. Particle size analysis

The particle size distribution of the milk powders was measured by laser diffraction using a particle size analyzer (PSA 1190 LD, Anton Paar

GmbH, Austria). Each test was performed in triplicate, and the mean particle size by volume was recorded.

### 2.3. Sample preparation for shear cell methodology

The shear cell set-up included a sample cup (18.9 mL) and the upper rotating geometry (Fig. 1). The sample preparation bench was used to gently load the powder into the sample cup, without excessive packing force or movement. A scraper bar was used to remove the excess powder and create a flat surface of powder across the top of the cup. On average, the cup held  $5.75 \pm 0.35$  g of milk protein powder and  $12.6 \pm 0.5$  g of calcium carbonate powder. The filled sample cup was placed on the rheometer platform and shear tested at room temperature (22 °C).

### 2.4. Shear cell measurements

An Anton Paar MCR302e Rheometer (Anton Paar, GmbH, Austria) with shear cell attachments was used for measuring flow properties of milk protein powders. The Rheocompass software (V1.30.1064) was used for analyzing data.

The measurements method consisted of two phases within each major section of the shear test: pre-shearing and shearing (Fig. 2). Pre-shearing was done to eliminate history of the powder samples. In this step, the powder sample was pre-sheared at a higher normal stress and subsequently sheared at a much lower normal stresses, yielding instantaneous powder flow. During the shearing process, the material's response was recorded as the shear stress needed to cause failure in the material upon applying constant normal stress. Prior to analyzing the milk protein samples, a certified reference (BCR-116 calcium carbonate powder) was used as the standard reference for the shear tests. The first round of testing with the BCR-116 calcium carbonate standard was performed with the default template (pre-shear normal stresses: 3, 6, and 9 kPa at 0.005 rpm) available within Rheocompass software. Subsequently, the milk protein powders were also subjected to the same shear testing parameters. The tests were consecutively conducted at three different pre-shear normal stresses, which spanned three action blocks in the software, each consisting of three shearing normal stresses. The same powder was used throughout each of these action blocks. Test results were expressed in terms of a ratio of maximum principal stress ( $\sigma_1$ ) to the unconfined yield strength ( $\sigma_c$ ) of the powder, also known as flow function coefficient ( $ffc$ ). Using the Mohr's circle, the yield loci of the powder were plotted, providing the framework for calculating the flow function coefficient ( $ffc$ ) for the powder samples.

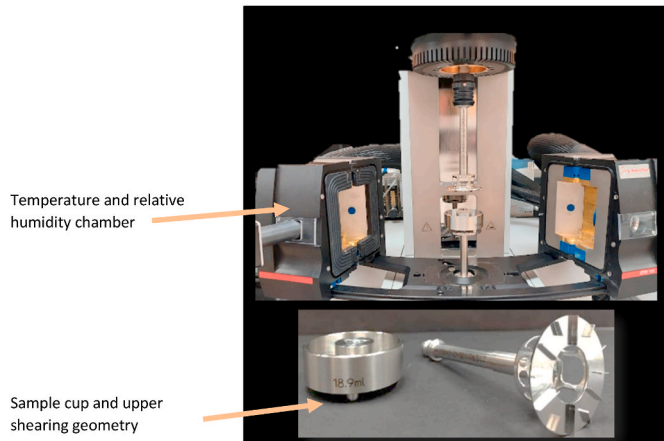


**Fig. 1.** Shear cell rheology cell set-up attached to MCR302e rheometer, equipped with temperature and relative humidity chamber.

### 2.5. Calculation of the flow function coefficient ( $ffc$ )

The Mohr's circle can be used to calculate the flow function coefficient by applying the Mohr-Coulomb model (Fig. 3). While the pre-shear points ( $\sigma_p$ ,  $\tau_p$ ) are gathered by the instrument software during the shear test, the Cohesion (C) is calculated as an intercept ( $\tau_1$ ) crossing y-axis using a linear regression line fitted through the yield loci. The angle of linearized yield locus ( $\alpha$ ) is the slope of the line connecting the yield loci and is affected in the manner by which the powder particles move past each other when subjected to a combination of the shear and normal stresses (Wang et al., 2016a). The Mohr-Coulomb model can be described in equation (1).

$$\tau = \sigma * \tan(\alpha) + \tau_1 \quad (1)$$

where  $\tau$  = shear stress (kPa),  $\sigma$  = normal stress (kPa),  $\tau_1$  = intercept of the linearized yield loci which is also called Cohesion and  $\alpha$  = angle of linearized yield locus.

The unconfined yield strength and consolidation stresses can be calculated using the following equations (2)–(4) as described in (Wang et al., 2016a).

$$\sigma_c = \tau_1 \cdot 2 * \tan\left[45 + \frac{\alpha}{2}\right] \quad (2)$$

$$\tau_1 = (1 + \sin \alpha) \left[ \frac{S - \sqrt{S^2 \sin^2 \alpha - (\tau_p^2 \cos^2 \alpha)}}{\cos^2 \alpha} \right] - \frac{\tau_1}{\tan \alpha} \quad (3)$$

$$S = \sigma_p + \frac{\tau_1}{\tan \alpha} \quad (4)$$

where,

$\sigma_1$  = consolidation stress

$\sigma_c$  = unconfined yield strength.

The flow function coefficient ( $ffc$ ) indicates the extent of flowability which is inversely related to cohesiveness of the powders. The  $ffc$  can be calculated from the values of the maximum principal stress and unconfined yield strength of the powder, as described in equation (5).

$$ffc = \frac{\sigma_1}{\sigma_c} \quad (5)$$

The range of the  $ffc$  determines whether a powder is cohesive or flowable. As described by Schulze (2008), an  $ffc$  of less than 1, indicates the powder is non-flowing, while an  $ffc$  between 1 and 2, indicates the powder sample is highly cohesive. At the same time, an  $ffc$  of 2–4, demonstrates cohesiveness in the sample, while an  $ffc$  in the range of 4–10, demonstrates easy-flowing characteristics. Lastly, an  $ffc$  greater than 10 is an indicator of high flowability of the sample.

### 2.6. Scanning electron microscopy (SEM)

Along with the particle size, the shape of the particles can also have an impact on the flow behavior of the powders (Juliano and Barboza-Cánovas, 2010). To assess the particle morphology, a scanning electron microscope was used (SEM, FEI Quanta 650 F, Thermo Scientific Quanta, Hillsboro, OR) under high vacuum (accelerating voltage: 15 kV, spot size: 2, detector: ETD). Powder samples were placed on aluminum stubs fixed with carbon tabs, flushed with nitrogen for 10 s and sputter coated with 10 nm of gold and palladium sputter coater (Q 150 V, Quorum technologies, Laughton, East Sussex, UK). All the samples were analyzed in duplicate ( $N > 30$ ).

### 2.7. Statistical analysis

The significant differences due to various treatments were analyzed using a one-way ANOVA in OriginPro (2021) for comparing means. The

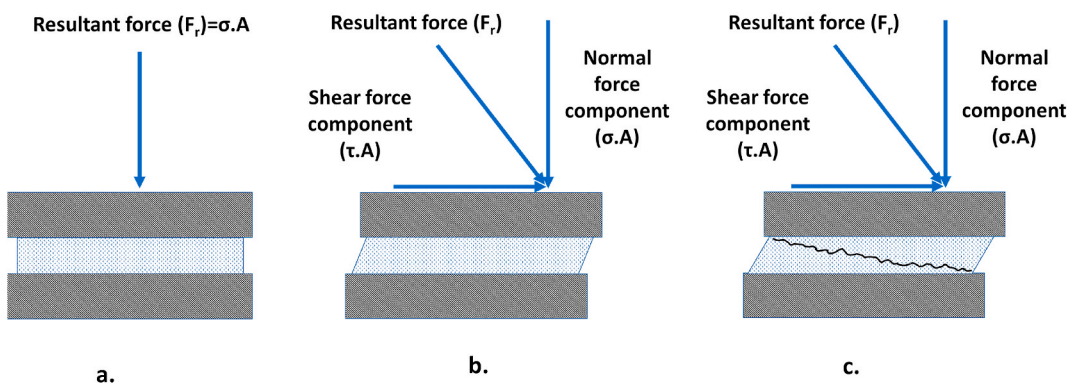


**Fig. 2.** Schematic diagram representing force resolution during shear cell testing; a. Bulk solid under rest conditions, b. pre-shear conditions, c. shear-to-failure condition.

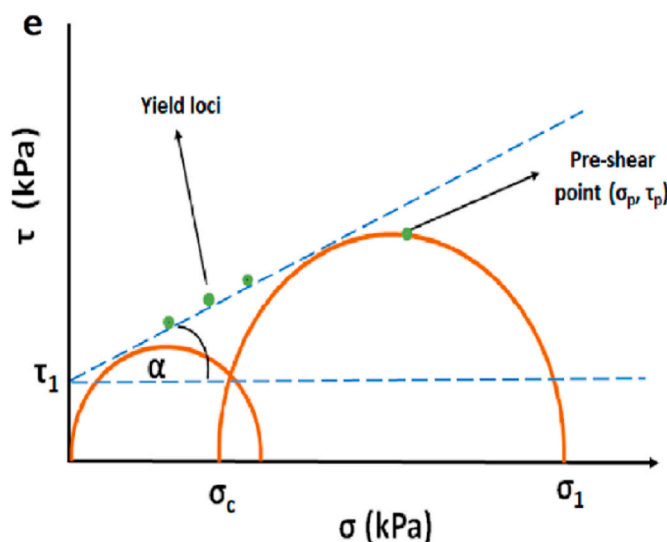


**Fig. 3.** Schematic representation of yield locus and pre-shear point. Mohr's circle. Mohr circle analysis can be used to derive cohesion ( $\tau_1$ ), unconfined yield strength ( $\sigma_c$ ), and major principal stress ( $\sigma_1$ ).

mean values of each parameter were compared for significant differences using Tukey's HSD post Hoc test at a 5% of level of significance.

### 3. Results and discussion

#### 3.1. Physicochemical properties

##### 3.1.1. Bulk density and water activity

Physicochemical properties of milk protein powders are presented in Table 1. Despite of slightly larger particle size, MPC 80 had higher bulk density and particle density than MPI 85, which can be attributed to the

slightly higher moisture content, lactose, and ash content. Purification of proteins during ultrafiltration is achieved by adding water to the retentate through diafiltration steps which washes out lactose and mineral. MPC 80 powder had a higher moisture, water activity, fat, and lactose content than the MPI 85 powder.

##### 3.1.2. Particle size

In this study, the particle size of the MPC 80 and the MPI 85 was 77.7  $\mu\text{m}$  and 52.5  $\mu\text{m}$ , respectively. Particle size of both milk protein powders was higher than ( $P < 0.05$ ) the BCR-116 calcium carbonate standard which had a mean particle size of 4.03  $\mu\text{m}$  (Table 1; Fig. 4). The particle size can have a direct impact on the powder flowability. Prior research has shown that the particle size of milk protein powders is inversely proportional to the specific surface area (SSA) for powders with similar protein concentrations (Silva and O'Mahony, 2017). Increased surface area will create more friction between particles. Milk protein concentrate powders with a larger particle size (particle diameter: 160  $\mu\text{m}$ ), and higher protein content (70%), had a higher flow index of 8.7, classifying it as free-flowing. We also observed a similar trend with respect to particle size and  $ffc$  values of  $\text{CaCO}_3$  standard and milk protein powders (Tables 1 and 3).

Crowley et al. (2014) noted that for milk protein powders composed of 80 and 85% protein, the particle size decreased with an increasing protein content. This aligns with the measurements in our study, where the MPI 85 powders had a smaller particle size (52.5  $\mu\text{m}$ ) than the MPC 80 powders (77.7  $\mu\text{m}$ ). We also observed a similar trend between the particle size and the specific surface area, with the latter being higher for the milk protein powders with 80 and 85% protein contents. This lowered their flowability due to a higher particle-particle interaction and greater friction between particles (Crowley et al., 2014).

##### 3.1.3. Particle morphology

There was a distinct difference in the morphological characteristics of the calcium carbonate standard compared to the milk protein powders. The calcium carbonate standard had smaller particles with flatter surfaces having sharp corners and irregular shape. In comparison to

**Table 1**  
Physicochemical properties of the powders.

| Powders | Moisture (%) | Fat (%) | Protein (%) | Lactose (%) | Ash (%) | Water Activity ( $a_w$ )  | Bulk density (g/mL) |                  | Particle density (g/mL) | D 10 ( $\mu\text{m}$ )  | D 50 ( $\mu\text{m}$ )  | D 90 ( $\mu\text{m}$ )   | Mean Size Volume D [4,3] ( $\mu\text{m}$ ) |
|---------|--------------|---------|-------------|-------------|---------|---------------------------|---------------------|------------------|-------------------------|-------------------------|-------------------------|--------------------------|--|
|         |              |         |             |             |         |                           | Loose bulk density  | Tap Bulk density |                         |                         |                         |                          |  |
| MPC 80  | 5.50         | 0.92    | 81.0        | 5.38        | 7.00    | 0.19 ± 0.003 <sup>a</sup> | 0.31                | 0.43             | 0.85                    | 21.1 ± 0.4 <sup>a</sup> | 58.1 ± 0.2 <sup>a</sup> | 139.5 ± 3.7 <sup>a</sup> | 77.7 ± 0.7 <sup>a</sup>                    |
| MPI 85  | 5.04         | 0.82    | 86.7        | 5.12        | 6.63    | 0.15 ± 0.009 <sup>b</sup> | 0.29                | 0.38             | 0.78                    | 7.85 ± 0.3 <sup>b</sup> | 46.3 ± 0.6 <sup>b</sup> | 96.2 ± 0.6 <sup>b</sup>  | 52.5 ± 0.6 <sup>b</sup>                    |

Different lowercase superscripts show significant differences ( $P < 0.05$ ) within the column.

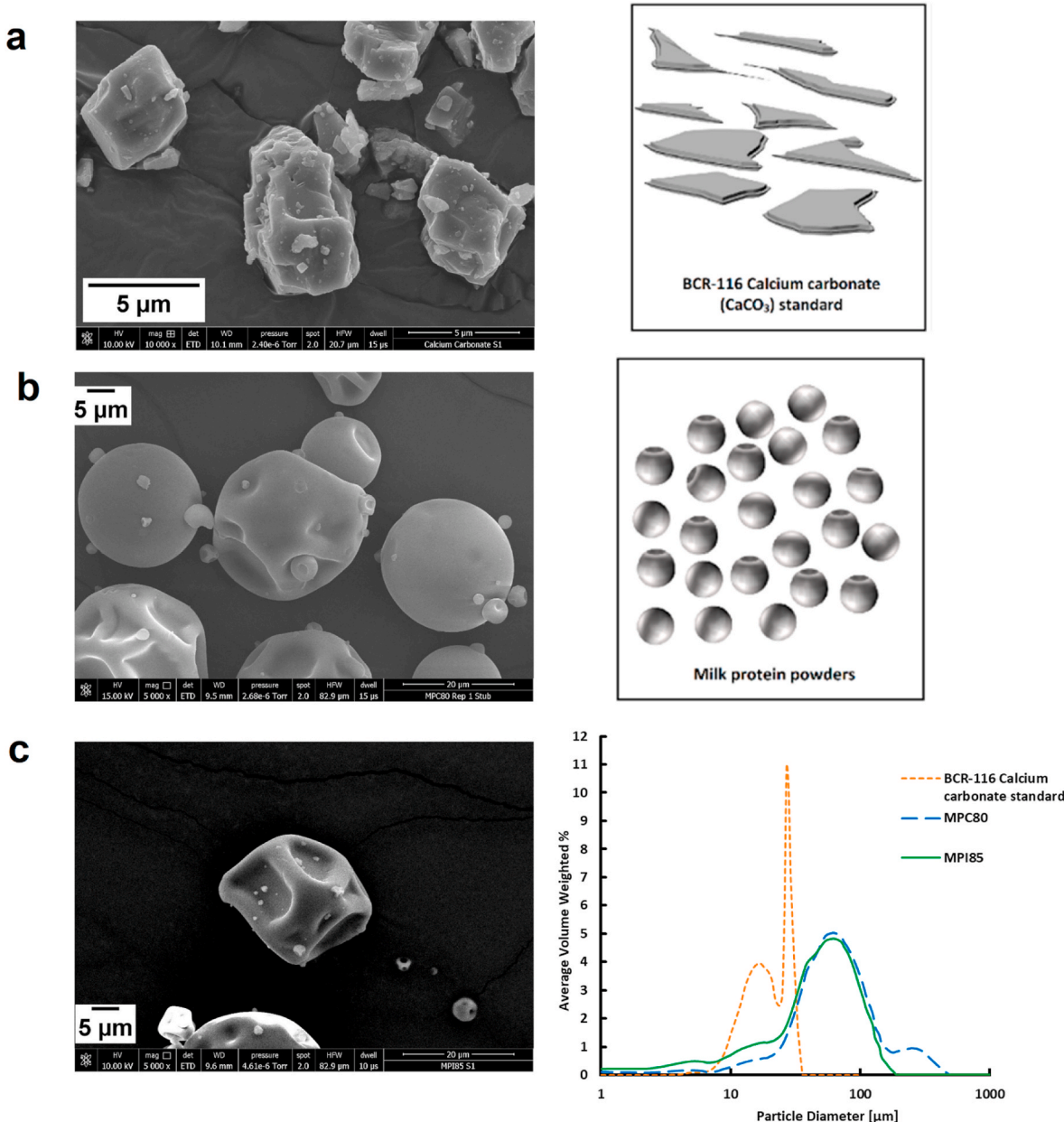


**Fig. 4.** Scanning electron micrographs of powders with schematics for particle shape; BCR-116 calcium carbonate standard (a), MPC 80 (b) and MPI 85 (c). Volume weighted particle size distribution of three powders is also depicted.

calcium carbonate, both MPC 80 and MPI 85 powders had a relatively globular shape (Fig. 4 b, c). The MPI 85 had a smaller particle size, with a large number of wrinkled marks on the surface than the MPC 80 powders. Both the milk protein powders had several smaller particles attached to the larger particle. These could be smaller protein structures that may have been formed during the spray-drying process.

Prior studies have shown that the milk powders can have both a smooth and spherical surface, as well as grooved, or wrinkled surfaces (de Jesus Silva et al., 2021; Ji et al., 2016; Maidannyk et al., 2020; Silva and O'Mahony, 2017). These grooves could have resulted during the spray-drying process itself (de Jesus Silva et al., 2021).

### 3.2. Shear cell testing with a set of 3, 6 and 9 kPa pre-shear normal stress

#### 3.2.1. BCR-116 calcium carbonate standard – 3, 6, and 9 kPa

Shear-to-failure diagrams of the calcium carbonate standard at three pre-shear normal stresses are presented in Fig. 5. It is clearly shown in

the figure that after achieving critically consolidated state on each pre-shear normal stress (3, 6, 9 kPa), the sample was subjected to much lower shearing normal stress. The BCR-116 calcium carbonate powder showed visible shear-to-fail peaks on each shearing normal stress on each pre-shear consolidation stress at a shear speed of 0.005 rpm. Throughout the test, the shear-to-failure points incrementally increased with the increase in applied normal stress (both pre-shear and shearing) (Table 2). The reference powder was classified as cohesive at 3 and 6 kPa, as indicated by the *ffc* values ranging from 2.1 to 3.5 (Schulze, 2008). Cohesive nature of this powder can be attributed to the smaller particle size and irregular shape of the powder particles as described in section 3.1.2 and 3.1.3.

The *ffc* values increased with the applied pre-shear normal and shearing normal stresses during testing (Table 2). The presence of shear-to-failure points on stress diagrams was shown as the response of the powder to the applied stresses, measured in terms of a distinct yield point or failure point, at which the powder yields and starts flowing. The

**Table 2**Flow function coefficients (*ffc*) of the milk protein powders and calcium carbonate at 3, 6 and 9 kPa pre-shear normal stress intervals, with shear speed of 0.005 rpm.

| Powders                            | Pre-shear normal stress (kPa) | Shearing normal stresses (kPa) | <i>ffc</i> values | Coefficient of Variance | Remarks  |
|------------------------------------|-------------------------------|--------------------------------|-------------------|-------------------------|--|
| BCR-116 calcium carbonate standard | 3                             | 0.9, 1.65, 2.4                 | 2.1 ± 0.1         | 3.7                     | Consistent shear failure point and absence of stick-slip phenomenon.                         |
|                                    | 6                             | 1.8, 3.3, 4.8                  | 3.5 ± 0.1         | 3.4                     | Sample classified as cohesive at 3, 6 kPa and easy flowing at 9 kPa.                         |
|                                    | 9                             | 2.7, 4.95, 7.2                 | 4.9 ± 0.2         | 4.2                     |  |
| MPC 80                             | 3                             | 0.9, 1.65, 2.4                 | 6.6               | nd                      | Only one replicate successful, inconsistent <i>ffc</i> values, stick-slip phenomenon present |
|                                    | 6                             | 1.8, 3.3, 4.8                  | 10.3              | nd                      | Two replicates possible, inconsistent <i>ffc</i> values, stick-slip phenomenon present       |
| MPI 85                             | 9                             | 2.7, 4.95, 7.2                 | 8.4               | nd                      | Two replicates possible, inconsistent <i>ffc</i> values                                      |
|                                    | 3                             | 0.9, 1.65, 2.4                 | 8.7               | nd                      | Lack of defined shear-to-failure points, classified as free flowing throughout each interval |
|                                    | 6                             | 1.8, 3.3, 4.8                  | 11.3              | nd                      | Inconsistent <i>ffc</i> values   |
|                                    | 9                             | 2.7, 4.95, 7.2                 | 10.6              | nd                      | Lack of defined shear-to-failure points  |

The range of *ffc* values used in the classification of flowability of powders were as obtained from [Schulze \(2008\)](#). Free flowing *ffc* >10; Easy flowing 4 < *ffc* <10; Cohesive 2 < *ffc* <4; Very cohesive 1 < *ffc* <2; not flowing *ffc* <1. The *ffc* values are presented as Mean ± SD for Calcium Carbonate.

nd = not done.

occurrence of these discrete yield points is critical for predicting the exact shear stress at which the sample begins to flow, thereby paving way for using the shear cell with less cohesive dairy powders, such as MPC 80 and MPI 85. It is clearly visible that set of 3, 6, 9 kPa of pre-shear consolidation stress worked well for calcium carbonate power, providing with very consistent *ffc* values.

### 3.2.2. MPC 80 and MPI 85

The next step in the shear cell measurements was to subject the milk protein powders (MPC 80 and MPI 85) to similar stress conditions as the standard (pre-shear 3, 6, and 9 kPa at a shear speed of 0.005). Neither of these powders showed a distinctive shear-to-failure peak at any of the applied shearing normal stresses (Table 2), in contrast to the standard calcium carbonate ([Fig. 5](#)). Absence of shear-to-failure point can be attributed to the fact that consolidation stresses in both pre-shear and shearing were so high that they were causing instant flow of the powder particles ([Schulze, 2008](#)). This can be attributed to the fact both powders had larger and smoother particles than calcium carbonate, facilitating incipient flow of these powders ([Fig. 4](#)). Both powders exhibited

stick-slip behavior (fluctuating shear stress). Because of these fluctuations, or noises, distinctive shear-to-failure peaks were not present. Interestingly, MPC 80 powders experienced more of these fluctuations than MPI 85, as seen in [Fig. 5](#) (b) and (c).

Further, the *ffc* values of both milk protein powders were inconsistent and were obtained only for less than three replicates (Table 2). The *ffc* increased with the applied pre-shear normal stresses until 6 kPa, like the phenomenon observed in the case of the calcium carbonate standard. However, the *ffc* value decreased when the powders were subjected to the 9 kPa pre-shear normal stresses. This decrease in *ffc* values can be attributed to the fact that at higher normal stress levels powders tend to flow instantly, and therefore do not show distinctive failure points. Along with the large variations in the shear-to-failure peaks and the occasional absence of such peaks made methods of determining *ffc* values of these powders highly challenging, thus hindering further analysis of the milk protein powders when tested at higher consolidation stresses.

Prior research has shown that when powders are exposed to higher pre-shear or shearing normal stress, they tend to undergo stick-slip friction ([Bagga et al., 2012; Blau, 2009; Kamath et al., 1994; Lubert and de Ryck, 2001; Schulze, 2008](#)). Stick-slip happens when the powder particles move past each other in a way that creates intermittent relative friction within the sample or between particle and equipment surface ([Bagga et al., 2012; Blau, 2009; Pant et al., 2020; Schulze, 2008](#)). This phenomenon is often explained by alternating slipping and sticking tendency of contact surfaces. Stick-slip is usually observed within the materials with larger particles with less cohesivity, such as sand, ash, and organic materials, including food powder and polymers. Stick-slip phenomenon is also associated with static and kinematic friction ([Bagga et al., 2012; Blau, 2009; Schulze, 2008](#)) and can occur between the particles themselves, or on the contact surfaces of the solid materials when handled as a bulk system. Switch over from static (high) to kinematic (lower) friction causes sticking and slipping tendency. The stick-slip events sensed by the rheometer are expressed by jumps or sawtooth patterns seen in the shear stress profile, as the upper geometry moves within the powder ([Fig. 5](#)). These sawtooth patterns can cause an error in the accurate estimation of the shear-to-failure stress which can cause error in the Mohr's circle analysis. Therefore, in order to ensure reliable measurement of *ffc* values, stick-slip effect needs to be minimized as much as possible.

The mechanical behavior of granular materials such as powders depends on the particle size, arrangement of particles, amount of interstitial air present between particles, porosity, and surface characteristics of the powder particles ([Roussel, 2005](#)). Changes in the internal

**Table 3**Flow function coefficients (*ffc*) of the milk protein powders at 1, 3 and 6 kPa pre-shear normal stress intervals.

| Powders | Shear speed (rpm) | <i>ffc</i>              |                         |                          | Remarks   |
|---------|-------------------|-------------------------|-------------------------|--------------------------|---|
|         |                   | 1 kPa                   | 3 kPa                   | 6 kPa                    |   |
| MPC 80  | 0.003             | 3.5 ± 0.5 <sup>a</sup>  | 12.1 ± 6.1 <sup>c</sup> | 6.5 ± 3.8 <sup>d</sup>   | Lack of defined shear-to-failure points                                 |
|         | 0.005             | 4.6 ± 0.4 <sup>b</sup>  | 10.2 ± 4.2 <sup>c</sup> | 9.4 ± 2.2 <sup>d</sup>   | Inaccurate shear-to-failure points                                      |
|         | 0.006             | 4.6 ± 0.4 <sup>bA</sup> | 7.6 ± 1.2 <sup>cB</sup> | 20.3 ± 6.2 <sup>dc</sup> | Reduced stick-slip, definitive shear-to-failure points in each interval |
|         | 0.009             | 4.3 ± 0.3 <sup>b</sup>  | 8.4 ± 1.1 <sup>c</sup>  | 48.9 ± 60.1 <sup>d</sup> | Inaccurate shear-to-failure points                                      |
| MPI 85  | 0.006             | 3.7 ± 0.5 <sup>A</sup>  | 6.7 ± 0.8 <sup>B</sup>  | 9.2 ± 1.1 <sup>C</sup>   | Definitive shear-to-failure points in each interval                     |

The range of *ffc* values used in the classification of flowability of powders were as obtained from [Schulze \(2008\)](#). Free flowing *ffc* >10; Easy flowing 4 < *ffc* <10; Cohesive 2 < *ffc* <4; Very cohesive 1 < *ffc* <2; not flowing *ffc* <1. Shearing normal stress values were varied according to pre-shear normal stress values i.e. 0.2, 0.6, 1.2 kPa; 0.4, 1.2, 2.4; and 0.6, 1.8, 3.6 at 1.0, 3, and 6 kPa of pre-shear normal stresses, respectively. The *ffc* values are presented as Mean ± SD. Different lowercase superscripts show significant differences ( $P < 0.05$ ) between *ffc* values obtained using different shear speeds at a corresponding pre-shear normal stress. Uppercase subscripts show significant difference ( $P < 0.05$ ) between MPC 80 and MPI 85 at the shear speed of 0.006 rpm.

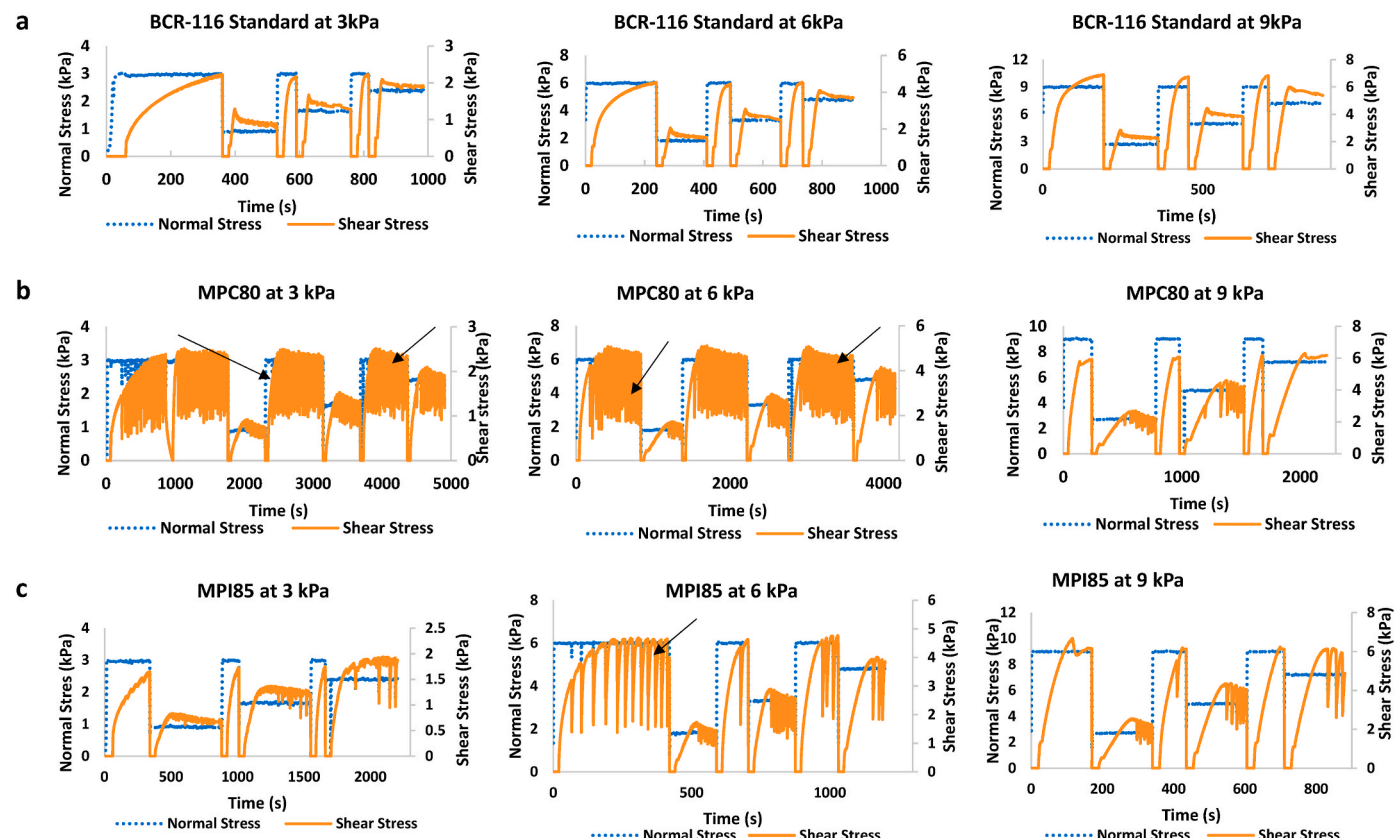


**Fig. 5.** The shear failure diagrams of the powders at 3, 6, 9, kPa pre-shear normal stresses with a, b and c representing the BCR-116 calcium carbonate standard, MPC 80 and MPI 85, respectively. All the tests were conducted in triplicate. However, single set of the data presented in this figure to clearly indicate presence of stick slip events. Arrows indicates presence of stick-slip phenomenon in the case of milk protein samples. Absence of shear to failure points can also be seen at 6 and 9 kPa pre-shear normal stresses.

arrangements of the particles or their movement during shearing and/or applying normal stress can influence flow behavior of bulk powders. During sticking, powder particles are close packed at the interface, exhibiting higher shear strength (Cain et al., 2001). A periodic dilatancy at the bulk level is observed when powder particles slide over each other creating more void space and minimizing frictional force (Powrie, 2017). Roussel (2005) suggested that stick-slip behavior during shearing is a manifestation of formation of columns or chains supporting load, if it collapses there is a drop in the stress. This tendency of stick-slip can decrease with an increase in the particles size, but this is mostly related to contact points and friction between the particles, rather than the size. In our case, we observed the standard calcium carbonate with a mean particle size of 4.03  $\mu\text{m}$  showed a reduced or low stick-slip tendency as compared to the milk protein powders with a higher particle size (Table 1). This could be due to smaller size and the shape of calcium carbonate particles compared to the milk protein powders. The scanning electron micrographs of the calcium carbonate presented a flat surface with an irregular shape of the particulates. This morphology may have contributed to its added cohesiveness compared to the spherically shaped milk protein powders (Fig. 4). Moreover,  $\text{CaCO}_3$  particles have weak attractive interactions such as van der Waals forces which contributes to cohesiveness (Schulze, 2008). At the same time, the specific morphology of the calcium carbonate also indicates why these samples worked so well with the default protocol i.e., 3, 6, 9 kPa pre-shear consolidation stresses. However, this template did not work for milk protein powder samples because of their round shape and larger particle size (Table 1) causing instant failure or flow of the samples even in the pre-shearing phase. This led to non-reliable shear-to-failure points needed for consistent values of  $ff$ . Therefore, the above protocol which worked

with the standard did not work well with the milk powder.

Ideally, at each shearing phase, irrespective of the amount of pre-shear normal stress employed (3, 6, and 9 kPa), the powder should exhibit definite shear-to-failure peaks or yield points. At a given pre-shear normal stress, three shear-to-failure peaks constitute the yield loci of the powder sample. At the end of the test, we observed three separate yield points, one from each major pre-shear interval. These three yield points formed the basis for constructing the Mohr's circle and subsequent  $ff$  calculations. Inconsistent shear-to-failure point, induced by the frequent stick-slip or due to instant flow, especially with 9 kPa, caused errors in determining these points, preventing the accurate depiction of the associated Mohr's circle. Milk protein powders tend to be more flowable than other powders. When used in the shear cell, they did not experience failure in the shearing phase. This could be due to higher pre-shear normal stresses which may have already initiated the incipient flow even during the pre-shearing stage and contributed towards the stick-slip, causing inconsistencies in the shear-to-failure points at each consolidation point. Teunou et al. (1999) concluded that, pre-shear normal stresses larger than 8 kPa can cause invalidity in the results, and hence must be avoided for food powders.

### 3.2.3. Testing with 1, 3, and 6 kPa pre-shear normal stress and reduced shearing normal stresses

Once it was apparent that the protein powders did not exhibit distinctive shear-to-failure peaks like the calcium carbonate standard at 3, 6, and 9 kPa, our next strategy was to reduce the pre-shear normal stresses to 1, 3, and 6 kPa and shearing normal stresses by almost half values at each of the pre-shear normal stresses (Tables 2 and 3) and assess their effect on reducing the instant failure of the powder and stick-

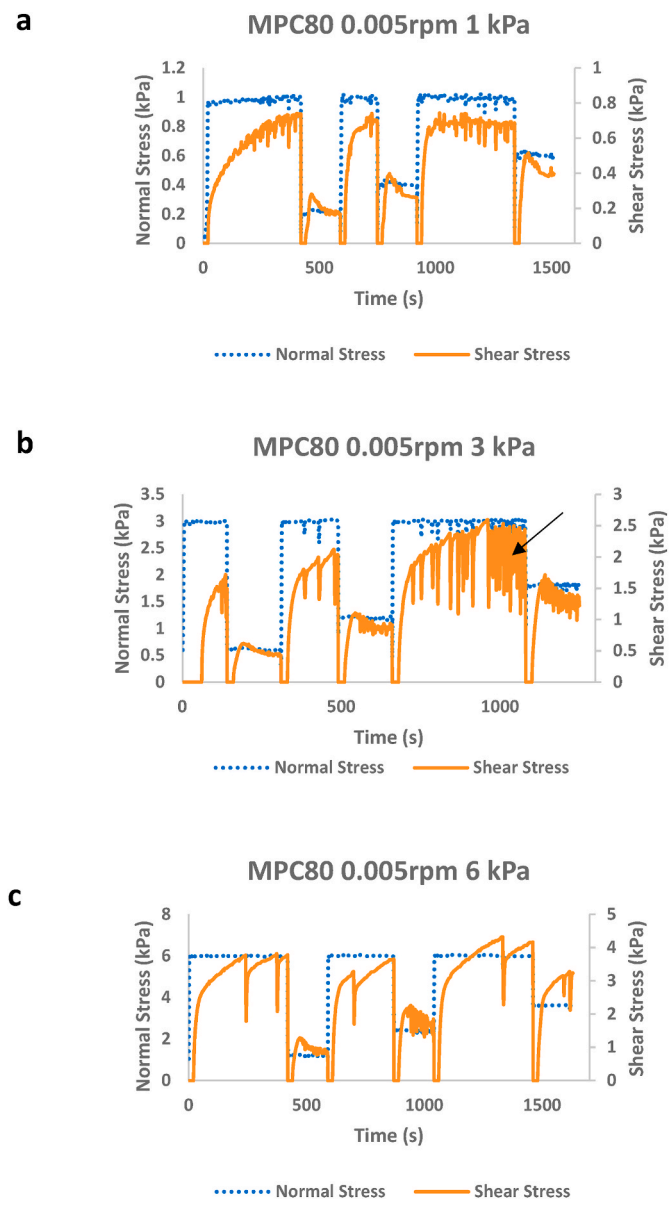


**Fig. 6.** Shear failure behavior of MPC 80 powder exposed to 1,3,6 kPa pre-shear normal stresses at 0.005 rpm. All the tests were conducted in triplicate however, data presented here represent one test replicate.

slip type fluctuations on the shear-failure curves. Fig. 6 presents the shear-to-failure peaks in the MPC 80 samples when subjected to the pre-shear normal stresses of 1, 3, and 6 kPa at lower shearing normal stresses (Table 3). The MPC 80 powder showed a lower stick-slip phenomenon at all the pre-shear intervals (1, 3, 6 kPa normal stress). It is clearly evident that lowering the pre-shear and shearing normal stresses significantly reduced stick-slip effect, eliminated instant failure of the bulk powder, making it possible to get accurate and reliable shear-to-failure points.

Previously, researchers have also observed a similar pattern with other dairy powders. Using shear cell analysis, Baggio et al. (2012) studied the effects of temperature on the rheological properties of skim milk, whole milk, and cream powders. The authors concluded that the amplitude of these stick-slip patterns can be minimized by lowering the consolidation stresses during pre-shear and shearing phases.

#### 3.2.4. Impact of the measurement point duration on shear-failure peaks

Fig. 7 presents the shear-failure curves acquired at 0.5 and 2 s data capture intervals. We observed a contrast between the two acquisition

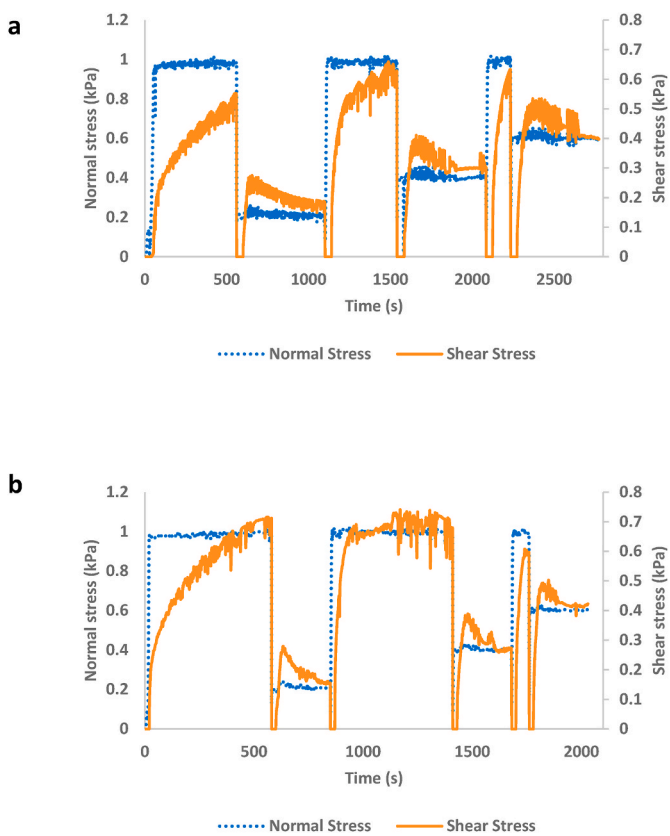


**Fig. 7.** Shear failure in MPC 80 powders at 0.003 rpm and 1 kPa pre-shear normal stresses; a and b represent data acquired at 0.5 and 2 s per interval, respectively. All the tests were conducted in triplicate however, data presented here represent one test replicate.

intervals (measurement point durations) adopted for collecting the points during the shear test measurements. When data was gathered every 0.5 s, there was an increase of stick-slip phenomena which was significantly reduced with 2 s measurement point duration. At 2 s interval the sawtooth patterns were less prevalent. More frequent data capturing leads to insufficient measurement duration, giving less chance for stress dissipation. Shorter measurement duration does not allow attainment of steady state, leaving transient effects (Sharma et al., 2015). To obtain reliable and accurate shear-to-failure points, it is important to give enough time for stress or strain loading during pre-shearing phase for attaining steady state conditions. This helps with alignment of particles on the surface, forming a cohesive and an elastic bed. During shearing phase, a relative motion between the particles and the contact surface is activated which causes eventual failure (incipient flow) of the material (Schulze, 2008). This is achieved by simultaneously applying normal and shear stresses.

As explained previously, the milk protein powders were more flowable or less cohesive than the calcium carbonate standard. Therefore, 0.5 s data capturing interval was enough for attaining steady flow for CaCO<sub>3</sub> standard but was not for the more flowable milk protein powders.

Since the standard was more cohesive than MPC 80, a shorter measurement point duration worked well since the stress curves showed clear shear-to-failure points. However, in the case of MPC 80, the increased flowability may have reduced the time required for the powder particles to attain a steady state and make a compact bed at the interface. As a result, the shear-to-failure peaks for the MPC 80 powders contained a higher number of stick-slip points. However, when the same powders were measured at 2 s interval, we observed a marked improvement in the shear-to-failure peaks (Fig. 7). We attribute this to

attaining steady state and formation of cohesive bed at interface, ready for the failure in the shearing phase.

### 3.2.5. Effects of the rotation speed

The powders were subjected to a range of shear speeds varying from 0.003 rpm to 0.009 rpm to assess the impact of shear speed. Fig. 8 represents the effects of different shear rotation speeds on the powders at 1, 3, and 6 kPa pre-shear normal stresses. The variations in shear speeds resulted in several interesting phenomena. It is clearly evident in Fig. 5 that at low pre-shear normal stresses (1 kPa) shear-to-failure points can be observed clearly at all three rotational speeds. However, the powder samples did show clear shear-to-failure points at 0.003 rpm with 3 and 6 kPa pre-shear normal stresses, thus severely depleting the further use of the data (Fig. 8). With an increasing shear speed (0.009), the powder samples showed a distinctive shear-to-failure points at all three pre-shear normal stresses (1, 3, 6 kPa). However, at 6 kPa normal stress, anomalies were observed in pre-shearing steady state flow conditions. Extreme amounts of stick-slip events occurred in the 3 kPa section when sheared at 0.009 rpm. Frequency of stick-slip behavior depends upon the shear velocity and the nature of interactions within powder particles or between surface of a rigid body (Schulze, 2008). Usually stick-slip behavior is more prevalent where bulk solid moves across the equipment contact surface. Shear stress at steady state decreased with consecutive shearing intervals, indicating concomitant changes in the organization of powder particles. This resulted to inaccurate shear-to-failure points, not suitable for obtaining reliable *ffc* values (Table 3). The frequency and amplitude of stick-slip events were reduced with the increasing shear speeds (from 0.003 to 0.006) at 6 kPa pre-shear normal stress (Fig. 8).

The shear speed of 0.006 rpm gave most consistent and reliable data during pre-shear and shearing of the powder across all the pre-shear normal stresses. Therefore, *ffc* values obtained at 0.006 rpm were most consistent. Depending upon particle characteristics, their arrangement due to consolidation and shearing, extent of void spaces, the stress or strain dissipation in the bulk solids varies. Optimum shear speed ensures arrangement of these structural elements, therefore steady state, and incipient flow.

The shear speed effects and associated results observed in this study were consistent with the prior research where a higher stick-slip was observed at higher shear rates (Bagga et al., 2012; Schulze, 2008). This was due to the inability of the bulk solids to flow at a higher shear speed, thereby increasing the particle-particle interactions. We observed that the flowability of milk protein powders increased with the shear speed at the 1 and 6 kPa pre-shear intervals (Table 3). This could be due to the increasing energy associated with the higher shear speeds, which may have caused the powders to be more flowable (Table 3).

To validate the robustness of the revised shear cell test, the most optimum shear cell test conditions (1,3, 6 kPa pre-shear normal stress; 0.006 rpm shear speed and 2 s measurement point duration) were applied on the MPI 85 sample (Fig. 9.). The powder showed distinctive shear-to-failure peaks at all kPa pre-shear normal stresses, This assisted in the calculation of an accurate *ffc*. The protocol developed in this study can be applied to various dairy powders. More research is needed to understand the impact of other external factors such as moisture and temperature on the flow characteristics of dairy powders with varying composition.

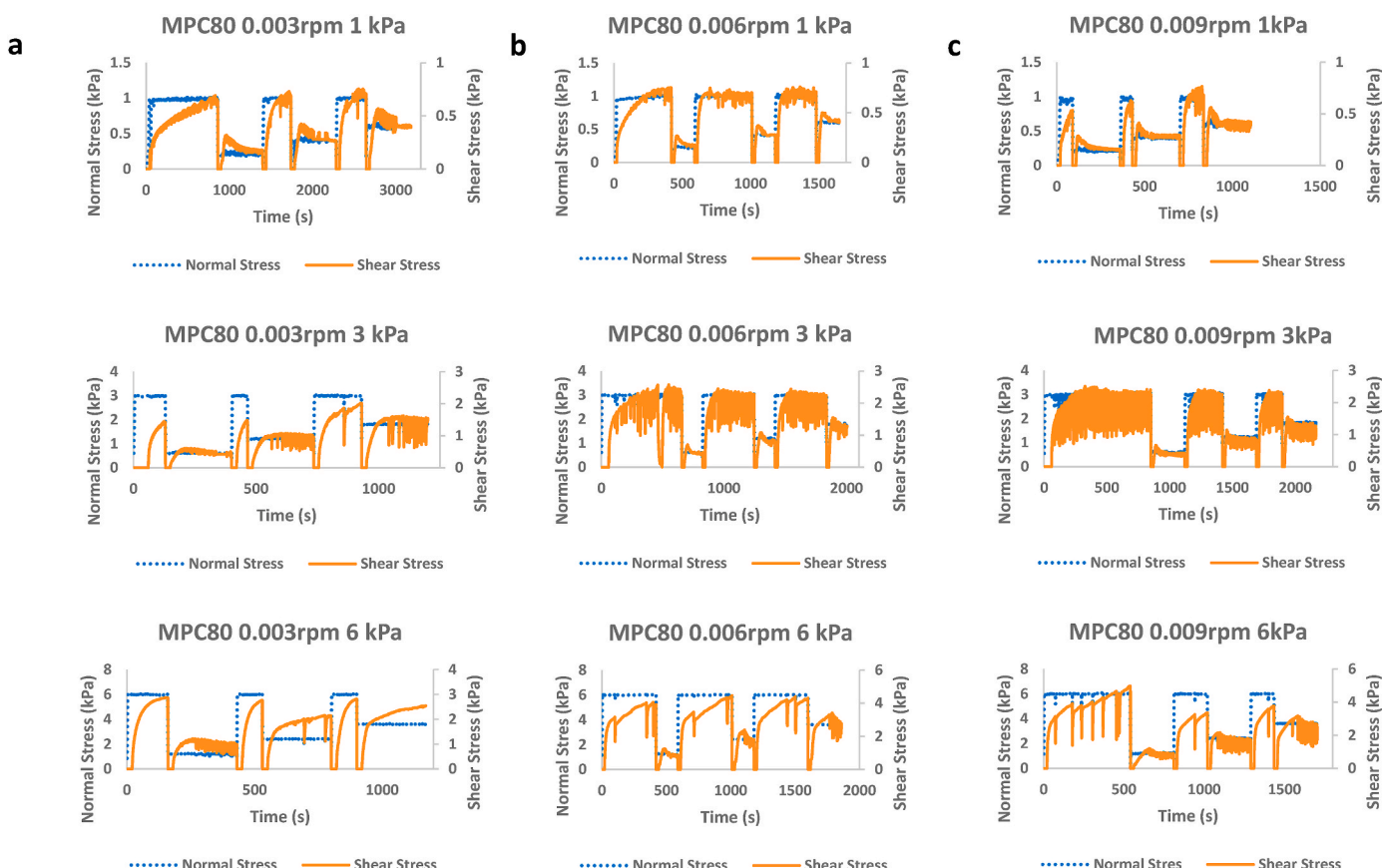
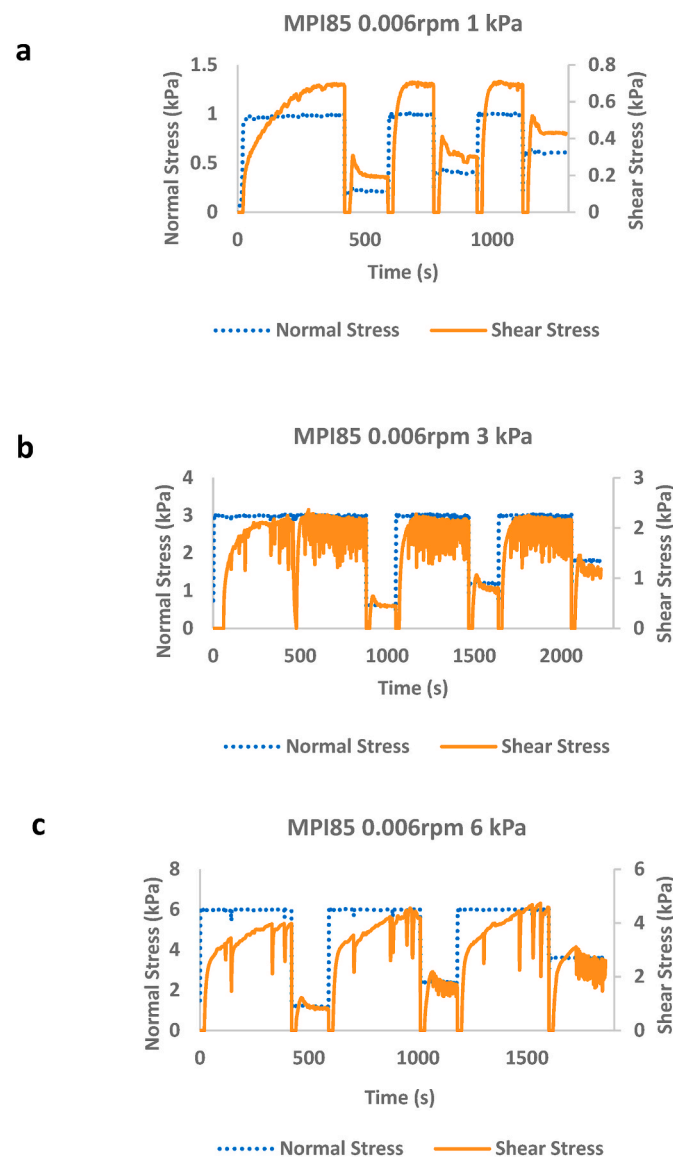


Fig. 8. Effect of shear speed on flow behavior of MPC 80 powder at 1, 3 and 6 kPa pre-shear normal stresses; a, b and c represent the shear speeds 0.003, 0.006 and 0.009 rpm, respectively. All the tests were conducted in triplicate however, data presented here represent one test replicate.



**Fig. 9.** Shear failure behavior of MPI 85 powders at 1, 3 and 6 kPa pre-shear normal stresses and 0.006 rpm. All the tests were conducted in triplicate however, data presented here represent one test replicate.

#### 4. Conclusion

The development of a shear cell method specifically for milk powders was critical to achieve *ffc* values that allowed for accurate assessment of the flow behavior. The milk protein powders behaved very differently compared to the inorganic calcium carbonate which is widely used as a standard for shear cell methodology. Factors such as powder density, particle size, and morphology contributed to shear behavior of the powders and influenced the specific test parameters required for each powder type. Lowering the pre-shear normal stresses from 3, 6, and 9 kPa to 1, 3, and 6 kPa and reducing shearing normal stresses minimized the stick-slip events in the MPC 80 and MPI 85 powders. A shear speed of 0.006 rpm worked best with both milk powders and provided consistent shear peaks from which an accurate *ffc* values could be obtained. Particle size and SEM measurements provided detailed information that was applicable in developing a greater understanding of the differences in the flow behaviors between sample types. The powders used in this study had substantial differences. This work clearly demonstrates the nature of organic vs inorganic powder samples when shear tested and reveals the need for a methodology that is effective and can be utilized to

characterize milk protein powders.

#### Credit author statement

Katelynn Palmer: Investigation, Methodology, Writing -Original Draft. Ashutos Parhi: Investigation, Methodology, Writing -Original Draft. Abhishek Shetty: Investigation, Methodology, Conceptualization, Writing – review & editing. Venkateswarlu Sunkesula: Investigation, Writing – review & editing. Prateek Sharma: Conceptualization, Methodology, Writing – review & editing, Supervision, Project administration, Funding acquisition.

#### Declaration of competing interest

The authors declare the following financial interests/personal relationships which may be considered as potential competing interests: Prateek Sharma reports financial support was provided by Dairy West.

#### Data availability

Data will be made available on request.

#### Acknowledgements

The authors would like thank Dr. FenAnn Shen, Manager, Microscopy Core Facility, Office of Research, Utah State University, Anton Paar USA, and the Idaho Milk Products for providing MPC 80 and MPI 85 samples for this study. Katelynn Palmer was supported by funding from the Building University-Industry Linkages through Learning and Discovery (BUILD) Dairy program of the Western Dairy Center (Utah State University, Logan) with financial support from Dairy West (Meridian, ID) and regional dairy processing companies. This research was also supported by the Utah Agricultural Experiment Station, Utah State University, and approved as journal paper number 9615.

#### References

- Akers, R.J., 1990. The Certification of a Limestone Powder for Jenike Shear Testing CRM-116. Loughborough Univ. of Technology, UK. BCR/163/90, Community Bureau of reference.
- Bagga, P., Brisson, G., Baldwin, A., Davies, C.E., 2012. Stick-slip behavior of dairy powders: temperature effects. *Powder Technol.* 223, 46–51. <https://doi.org/10.1016/j.powtec.2011.05.015>.
- Blau, P.J., 2009. *Friction Science and Technology: from Concepts to Applications*, second ed. CRC Press, Boca Raton, FL.
- Boiarkina, I., Sang, C., Depree, N., Prince-Pike, A., Yu, W., Wilson, D.I., Young, B.R., 2016. The significance of powder breakdown during conveying within industrial milk powder plants. *Adv. Powder Technol.* 27, 2363–2369. <https://doi.org/10.1016/j.apt.2016.10.019>.
- Cain, R.G., Page, N.W., Biggs, S., 2001. Microscopic and macroscopic aspects of stick-slip motion in granular shear. *Phys. Rev. E* 64, 016413. <https://doi.org/10.1103/PhysRevE.64.016413>.
- Carpin, M., Bertelsen, H., Dalberg, A., Bech, J.K., Risbo, J., Schuck, P., Jeantet, R., 2017. How does particle size influence caking in lactose powder? *J. Food Eng.* 209, 61–67. <https://doi.org/10.1016/j.jfoodeng.2017.04.006>.
- Chang, S.-Y., Li, S.W., Kowsari, K., Shetty, A., Sorrells, L., Sen, K., Nagapudi, K., Chaudhuri, B., Ma, A.W.K., 2020. Binder-jet 3D printing of indomethacin-laden pharmaceutical dosage forms. *J. Pharmaceut. Sci.* 109, 3054–3063. <https://doi.org/10.1016/j.xphs.2020.06.027>.
- Crowley, S.V., Gazi, I., Kelly, A.L., Huppertz, T., O'Mahony, J.A., 2014. Influence of protein concentration on the physical characteristics and flow properties of milk protein concentrate powders. *J. Food Eng.* 135, 31–38. <https://doi.org/10.1016/j.jfoodeng.2014.03.005>.
- de Jesus Silva, G., Gonçalves, B.-H.R.F., Conceição, D.G., de Jesus, J.C., Vidigal, M.C.T. R., Simiqueli, A.A., Bonomo, R.C.F., Ferrão, S.P.B., 2021. Microstructural and rheological behavior of buffalo milk chocolates. *J. Food Sci. Technol.* <https://doi.org/10.1007/s13197-021-05042-3>.
- Foster, K.D., Brønlund, J.E., Paterson, A.H.J., Tony, 2005. The contribution of milk fat towards the caking of dairy powders. *Int. Dairy J.* 15, 85–91. <https://doi.org/10.1016/j.idairyj.2004.05.005>.
- Fournaise, T., Burgain, J., Perroud, C., Scher, J., Gaiani, C., Petit, J., 2020. Impact of formulation on reconstitution and flowability of spray-dried milk powders. *Powder Technol.* 372, 107–116. <https://doi.org/10.1016/j.powtec.2020.05.085>.
- Gaspard, S.J., Sharma, P., Fitzgerald, C., Tobin, J.T., O'Mahony, J.A., Kelly, A.L., Brodkorb, A., 2021. Influence of chaperone-like activity of caseinomacropéptide on

- the gelation behaviour of whey proteins at pH 6.4 and 7.2. *Food Hydrocolloids* 112, 106249. <https://doi.org/10.1016/j.foodhyd.2020.106249>.
- Hartig, J., Shetty, A., Conklin, D.R., Weimer, A.W., 2022. Aeration and cohesive effects on flowability in a vibrating powder conveyor. *Powder Technol.* 408, 117724. <https://doi.org/10.1016/j.powtec.2022.117724>.
- Iams, A.D., Gao, M.Z., Shetty, A., Palmer, T.A., 2022. Influence of particle size on powder rheology and effects on mass flow during directed energy deposition additive manufacturing. *Powder Technol.* 396, 316–326. <https://doi.org/10.1016/j.powtec.2021.10.059>.
- Jange, C.G., Taku, P., Peng, S., Dixon, M.P., Shetty, A., Ambrose, R.P.K., 2020. Cohesivity assessment of semi-crystalline and crystalline powders using a Warren Springs cohesion tester. *Powder Technol.* 371, 96–105. <https://doi.org/10.1016/j.powtec.2020.05.077>.
- Ji, J., Fitzpatrick, J., Cronin, K., Maguire, P., Zhang, H., Miao, S., 2016. Rehydration behaviours of high protein dairy powders: the influence of agglomeration on wettability, dispersibility and solubility. *Food Hydrocolloids* 58, 194–203. <https://doi.org/10.1016/j.foodhyd.2016.02.030>.
- Juliano, P., Barbosa-Cánovas, G.V., 2010. Food powders flowability characterization: theory, methods, and applications. *Annu. Rev. Food Sci. Technol.* 1, 211–239. <https://doi.org/10.1146/annurev.food.102308.124155>.
- Kamath, S., Puri, V.M., Manbeck, H.B., 1994. Flow property measurement using the Jenike cell for wheat flour at various moisture contents and consolidation times. *Powder Technol.* 81, 293–297. [https://doi.org/10.1016/0032-5910\(94\)02888-5](https://doi.org/10.1016/0032-5910(94)02888-5).
- Khalesi, M., FitzGerald, R.J., 2021. Investigation of the flowability, thermal stability and emulsification properties of two milk protein concentrates having different levels of native whey proteins. *Food Res. Int.* 147, 110576. <https://doi.org/10.1016/j.foodres.2021.110576>.
- Lubert, M., de Ryck, A., 2001. Slip events and dilatancy in a sheared fine noncohesive powder. *Phys. Rev.* 63, 021502. <https://doi.org/10.1103/PhysRevE.63.021502>.
- Maidannyk, V., McSweeney, D.J., Hogan, S.A., Miao, S., Montgomery, S., Auty, M.A.E., McCarthy, N.A., 2020. Water sorption and hydration in spray-dried milk protein powders: selected physicochemical properties. *Food Chem.* 304, 125418. <https://doi.org/10.1016/j.foodchem.2019.125418>.
- Mishra, I., Liu, P., Shetty, A., Hrenya, C.M., 2020. On the use of a powder rheometer to probe defluidization of cohesive particles. *Chem. Eng. Sci.* 214, 115422. <https://doi.org/10.1016/j.ces.2019.115422>.
- Mishra, I., Molnar, M.J., Hwang, M.Y., Shetty, A., Hrenya, C.M., 2022. Experimental validation of the extraction of a particle-particle cohesion model (square-force) from simple bulk measurements (defluidization in a rheometer). *Chem. Eng. Sci.* 259, 117782. <https://doi.org/10.1016/j.ces.2022.117782>.
- Pant, A., Ramana, G.V., Datta, M., 2020. Stick-slip behavior of dry fly ash. *Part. Sci. Technol.* 38, 605–616. <https://doi.org/10.1080/02726351.2019.1571543>.
- Parrella, L., Barletta, D., Boerefijn, R., Poletto, M., 2008. Comparison between a uniaxial compaction tester and a shear tester for the characterization of powder flowability. *KONA* 26, 178–189. <https://doi.org/10.14356/kona.2008016>.
- Powrie, W., 2017. *Soil Mechanics: Concepts and Applications*, third ed., third ed. CRC Press, London. <https://doi.org/10.1201/9781315275284>.
- Ramaraju, H., Landry, A.M., Sashidharan, S., Shetty, A., Crotts, S.J., Maher, K.O., Goudy, S.L., Hollister, S.J., 2022. Clinical grade manufacture of 3D printed patient specific biodegradable devices for pediatric airway support. *Biomaterials* 289, 121702. <https://doi.org/10.1016/j.biomaterials.2022.121702>.
- Roussel, L.E., 2005. Experimental investigation of stick-slip behavior in granular materials. Louisiana State University, Master's Theses. 4145. [https://digitalcommons.lsu.edu/gradschool\\_theses/4145](https://digitalcommons.lsu.edu/gradschool_theses/4145).
- Schulze, D., 2008. *Powders and Bulk Solids: Behavior, Characterization, Storage and Flow*. Springer, Berlin ; New York.
- Sharma, P., Dessev, T.T., Munro, P.A., Wiles, P.G., Gillies, G., Golding, M., James, B., Janssen, P., 2015. Measurement techniques for steady shear viscosity of Mozzarella-type cheeses at high shear rates and high temperature. *Int. Dairy J.* 47, 102–108. <https://doi.org/10.1016/j.idairyj.2015.03.005>.
- Silva, J.V.C., O'Mahony, J.A., 2017. Flowability and wetting behaviour of milk protein ingredients as influenced by powder composition, particle size and microstructure. *Int. J. Dairy Technol.* 70, 277–286. <https://doi.org/10.1111/1471-0307.12368>.
- Stavrou, A.G., Hare, C., Hassanpour, A., Wu, C.-Y., 2020. Investigation of powder flowability at low stresses: influence of particle size and size distribution. *Powder Technol.* 364, 98–114. <https://doi.org/10.1016/j.powtec.2020.01.068>.
- Stoklosa, A.M., Lipasek, R.A., Taylor, L.S., Mauer, L.J., 2012. Effects of storage conditions, formulation, and particle size on moisture sorption and flowability of powders: a study of deliquescent ingredient blends. *Food Res. Int.* 49, 783–791. <https://doi.org/10.1016/j.foodres.2012.09.034>.
- Teunou, E., Fitzpatrick, J.J., Synnott, E.C., 1999. Characterisation of food powder flowability. *J. Food Eng.* 7.
- Tuohy, J.J., 1989. Some physical properties of milk powders. *Ir. J. Food Sci. Technol.* 13, 141–152.
- Wang, Y., Koynov, S., Glasser, B.J., Muzzio, F.J., 2016a. A method to analyze shear cell data of powders measured under different initial consolidation stresses. *Powder Technol.* 294, 105–112. <https://doi.org/10.1016/j.powtec.2016.02.027>.
- Wang, Y., Snee, R.D., Meng, W., Muzzio, F.J., 2016b. Predicting flow behavior of pharmaceutical blends using shear cell methodology: a quality by design approach. *Powder Technol.* 294, 22–29. <https://doi.org/10.1016/j.powtec.2016.01.019>.
- Zhao, Y., Phalswal, P., Shetty, A., Ambrose, R.P.K., 2021. Effects of Powder Vibration and Time Consolidation on Soft and Hard Wheat Flour Properties. *KONA Powder and Particle Journal* advpub, 2021007. <https://doi.org/10.14356/kona.2021007>.